

SYSTEMATIC SHAKE TABLE TESTS OF EQUIPMENT ON CASTERS

C. Xu¹, Q. Ma², M. Kurata³ & S. Beskhyroun⁴

¹ PhD Candidate, Dept. of Civil & Environmental Engineering, The University of Auckland, NEW ZEALAND

cxu413@aucklanduni.ac.nz

² Senior Lecturer, Dept. of Civil & Environmental Engineering, The University of Auckland, NEW ZEALAND

q.ma@auckland.ac.nz

³ Associate Professor, Disaster Prevention Research Institute, Kyoto Univ., Kyoto 6110011, JAPAN

kurata.masahiro.5c@kyoto-u.ac.jp

⁴ Associate Professor, School of Future Environments, Auckland University of Technology, NEW ZEALAND

sherif.beskhyroun@aut.ac.nz

Abstract: *Understanding the motion of equipment on casters can reduce economic loss and ensure the continuing function of critical infrastructure following earthquakes. However, the 3-dimensional rolling problem is unintuitively complex, and it is difficult to extend current analytical techniques to model even simple realistic systems. This paper covers the experimental design and method of the shake table testing of a trolley with casters, simulating the seismic response of medical equipment in hospitals. The study involves conducting an extensive series of over 1,300 uniaxial shake table tests. These tests covered a range of factors including different wheel sizes, wheel materials, wheel and trolley orientations, caster locking configurations, as well as variations in trolley self-weights and centre of mass heights. The systematic shake table tests utilised sinusoidal ground motions with varying frequencies, varying amplitudes and recorded earthquake ground motions from past earthquakes. Trolley displacements, caster rotation and twist were recorded through a combination of motion capture system, traditional instrumentation (accelerometers), and video recording. The tests were successful, with both the measurement and video systems operating efficiently. The collected data from the shake table tests provide a wide basis for future parametric analysis concerning the impact of various factors on the seismic response of hospital equipment.*

1 Introduction

Damaged non-structural elements (NSEs) and building contents can cause significant economic losses and reduction of a building's overall functionality after earthquakes (Taghavi and Miranda, 2003; Mitrani-Reiser *et al.*, 2012). NSEs and building contents often make up a large portion of the overall investment in a building, particularly in medical facilities. In fact, as much as 90% of the investment in a medical facility can be attributed to these elements (Taghavi and Miranda, 2003). NSEs' seismic performance affects the continued functionality of medical facilities, which is especially critical shortly after an earthquake (Miranda *et al.*, 2012; Mayer and Boston, 2022). Damaged NSEs and displaced contents can hinder safe evacuation, posing risks to patients and staff, (Zhang *et al.*, 2012; Suzuki, Fukuda and Nakaji, 2014).

Past earthquake observations show that even if a building's structural systems suffered only minor damage, the NSE and contents may still be significantly damaged (see Figure 1) (Dhakal, 2010; FEMA, 2015). The economic losses due to NSEs damage are typically considerably higher than those that result from structural damage (Fajfar and Krawinkler, 2004; Filiatrault and Sullivan, 2014). In the 2010 Chile earthquake, around 62% of hospitals in the affected region experienced non-structural damage requiring repairs, and roughly 75% of elevators in hospitals were non-functional post-earthquake (Miranda *et al.*, 2012). Although researchers have achieved significant progress in understanding the seismic performance of NSEs and building contents after the 2010 earthquake, widespread damage was still observed in Wellington after the 2016 Kaikōura earthquake (Baird and Ferner, 2017).

The study of how objects with wheels respond to seismic activity is an important, yet relatively underexplored field. Medical equipment is one of the most critical systems when considering the earthquake vulnerability of hospitals (Myrtle *et al.*, 2005). Those equipment, including ICU monitoring systems, anaesthesia equipment, ventilators, and defibrillators, are usually on casters without any anchorage. Past earthquakes indicate freestanding equipment can be damaged by collisions or overturning (Ornthammarath *et al.*, 2018). Available studies on the seismic performance of contents in hospitals mainly focus on freestanding contents without casters (Dhakal *et al.*, 2016; Di Sarno *et al.*, 2019). Objects with casters exhibit distinctive seismic responses due to the ability of casters to roll and twist. (Wang, Dai and Ning, 2016).

Despite the common usage of casters in medical facilities, studies focused on this area are limited. Shake table test is the most used method for experimental simulations. Some notable experimental studies include:

- the testing of a typical full-scale B-ultrasound room with various contents with or without casters (Wang, Dai and Ning, 2016), .
- the full-scale tests of a five-story building with its top two floors fitted out as a surgery suite and an intensive care unit (Elide Pantoli *et al.*, 2013),
- the shake table tests of various medical equipment were tested for evaluation and recommendation of seismic restraints (Chai and Lin, 2011), and
- the shake table tests of medical equipment with locked and unlocked caster conditions (Nikfar and Konstantinidis, 2019).

These studies primarily tested specific common hospital room contents, experimental opportunity exists for a systematic investigation into the fundamental factors affecting rolling response, such as effects of altering mass distribution, wheel material, and casters locking conditions.

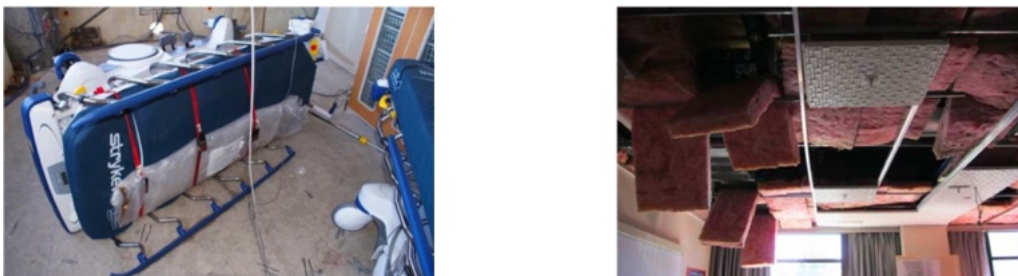


Figure 1 Overturned patient bed during shake table (left) (Elide Pantoli *et al.*, 2013) and ceiling tile damage in Christchurch Hospital (photo credit: Alan Bavis) (Jacques *et al.*, 2014)

This study is a significant investigation scrutinizing various factors influencing the seismic response of rolling objects. The test specimen involves a configurable trolley on casters, and a Motion Capture (MoCap) system recording the displacements and rotations of both the trolley and casters.

2 Shake table test design

This investigation conducted over 1,300 shake table test runs through sixteen different ground motion combinations. The experiments covered diverse configurations, including five caster types, six wheel angles, three trolley angles, three trolley self-weight, three centre of mass heights, and seven locking conditions.

2.1 Experiment specimen and floor covering

The experiment trolley rests on a 4mm thick vinyl floor covering (2mm gauge with a 2mm wearing layer), typically used in healthcare settings, which is in turns secured to plywood sheets fixed onto the shake table. The testing configuration is shown in Figure 2.



Figure 2 Testing specimen, vinyl flooring and MoCap cameras locations

2.1.1 The Trolley

The rolling specimen used in the shake table experiment is a steel trolley with a mass of 97 kg. The bare trolley measures 1100 x 550 x 1470 mm (BxDxH), and its centre of mass is situated at the planar geometric centre, 487 mm above the bottom of its base plate. A concrete block holder is added to the middle shelf, and an anti-overturning timber outrigger is attached below the base plate. The entire specimen has a mass of 122kg. The detailed dimension and mass information on the trolley is listed in Table 1. The trolley and casters are coated with a matte black finish to avoid conflict with the MoCap system. The trolley is shown in Figure 3.

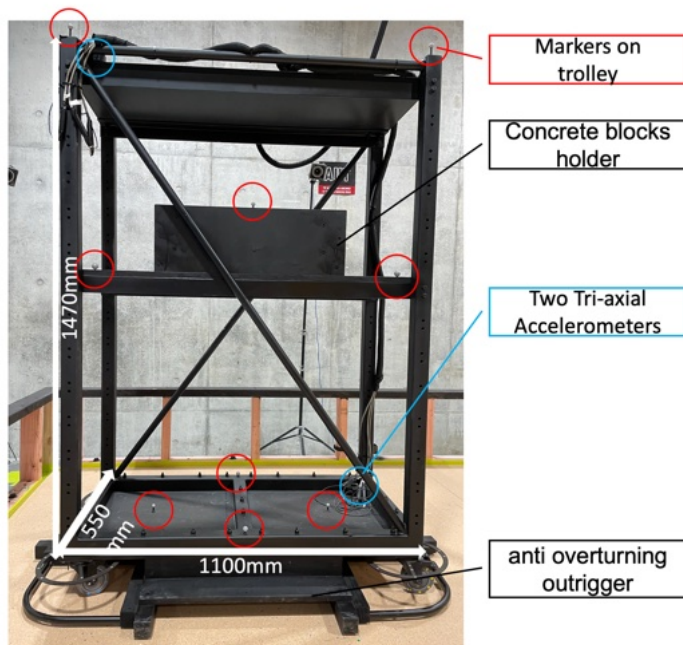


Figure 3 Trolley specimen used for shake table tests

Table 1 Trolley information.

Trolley parts	Mass (kg)
Mass - trolley body	97
Mass - anti-overturning outrigger	16
Mass - concrete blocks holder at middle shelf	9
Total	122

2.2 Data capture

2.2.1 Motion capture system

Motion capture (MoCap) system is utilized to record the three-dimensional displacement and rotation of both the trolley body and all casters. Six MoCap cameras are positioned around the shake table to capture the motion of several rigid bodies as defined in the system, outlined by reflective markers on the trolley. The MoCap system consists of six OptiTrack Prime 41 cameras and the software *Motive* conducts the computer vision calculations to obtain 3D tracking of the rigid bodies (OptiTrack, 2023). Using a MoCap system simplifies instrumentation as it does not influence the specimen's motion. A sample perspective view in *Motive* during data capturing is shown in Figure 4.

Reflective markers or stickers are attached to different locations of the trolley body as well as four casters to capture the twisting motion of casters. Laser cut discs with distinct pattern of reflective stickers are attached to the fork of each caster (see left and middle figure of Figure 5). For caster type 5 without a plate, a 3D printed holder was made to support the disk (see right figure of Figure 5). It is important to note that given the similarity of each caster, varying number of markers are strategically positioned with distinctive patterns and shapes to aid identification by *Motive* during the recording process.

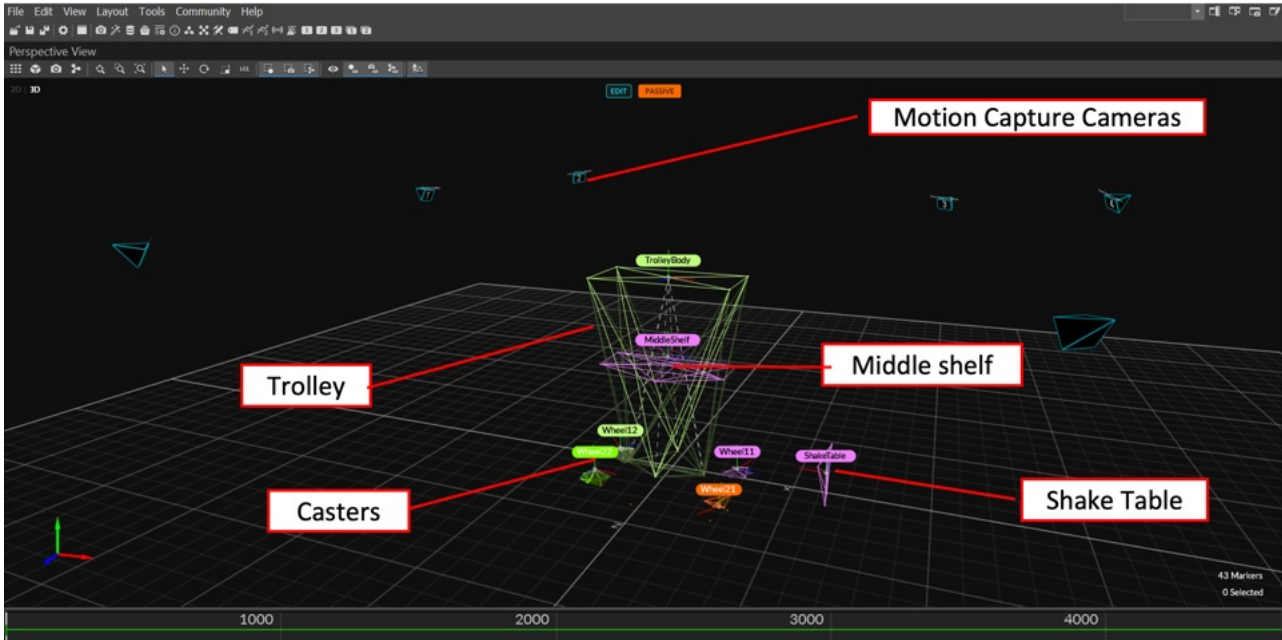


Figure 4 Perspective view in Motive generated by MoCap cameras during data capturing



Figure 5 Reflective markers on a disk fixed to caster's fork (left), and disk mounted to the plate-type caster (middle) or stem-type caster (right)

2.2.2 Accelerometers

Two tri-axial accelerometers are mounted at the top and the bottom of the trolley, respectively, as shown in the red circles in Figure 3. Likewise, a single-axis accelerometer is installed on the shake table to record its motion. To prevent any interference of the cables with the trolley's motion during testing, all cables were suspended above the trolley using an arm capable of rotation. The data obtained from these accelerometers was synchronized with the MoCap data via triggered sampling.

2.2.3 Video data

Due to limited MoCap camera availability, all the MoCap cameras were positioned at elevated angles to capture trolley body motion and caster twist. To additionally capture individual wheel rolling motion, six strategically positioned GoPro cameras recorded the testing. Four of these were directly focused on the lower part of the trolley to record wheel motion, while the remaining two, positioned at elevated angles, provided comprehensive coverage of the testing process, as shown in Figure 6.



Figure 6 Video captured by six GoPro cameras

2.3 Testing factors

The factors varied in the different test combinations are summarised in Table 2, and are further elaborated in this section.

Table 2 All factors tested during shake table tests.

Caster (Table 3)		Ground Motion (Table 5)	Payload (Table 4)		Orientation (Figure 10)		Lock caster arrangement
Wheel Material	Wheel Diameter (mm)		Additional mass	Mid shelf height	Wheel angle	Trolley angle	
Institutional Rubber, Polyurethane	100, 125	GM1-GM16	Low, Med, High	Low, Mid, High	0, 45, 90, 180, 0+45, 0+90	0, 45, 90	7 different arrangements as described in 2.3.3





2.3.1 Casters

Five different types of casters were used for shake table testing (see Figure 7). Detailed information on the selected casters is listed in Table 3. These casters include two wheel sizes, 100mm, and 125mm, and two wheel materials, institutional rubber and polyurethane. A special twin-wheel, stem mount, medical caster (caster 5) was also selected for the testing. The study also included testing a rigid caster (caster 2), which lacks the ability to twist, alongside two swivel casters equipped with the same type of wheel (caster 1). This configuration reflects another common caster setup encountered in real-world applications. Caster 1 serves as the control group, thereby facilitating comparative analysis with casters featuring distinct wheel dimensions and materials.



Figure 7 Casters used for shake table tests. #1 to #5 from left to right

Table 3 Caster information

	Caster code	Single or twin wheel	 Diameter (mm)	 Width (mm)	Rigid or Swivel	Wheel material	 Swivel offset (mm)	 Height (mm)
1	S4425B	S	100	32	S	Institutional Rubber	84	131
2	R4426	S	100	32	R	Institutional Rubber	-	131
3	S5525B	S	125	32	S	Institutional Rubber	100	160
4	S4422B	S	100	32	S	Polyurethane	84	131
5	S4312B Med	T	100	2x16	S	Polyurethane	80	123

2.3.2 Trolley self-weight and centre of mass height

The trolley was designed with a central shelf with a modifiable height. Either two or four concrete blocks, each with a mass of 13.6kg, were added to the central shelf as mass variation for the systems (see Figure 8). These adjustments result in three levels of the trolley self-weight, labelled as “L,” “M,” and “H” (see Table 4). The centre of mass can also be adjusted by altering the position of the middle shelf, denoted as “L,” “M,” and “H” from left to right in Figure 9.



Figure 8 Added concrete blocks to change the specimen's self weight

Table 4 Three trolley's self-weight levels.

Trolley mass	Concrete block mass	Total mass (kg)	Self weight level
122 kg	0	122	L
	2 x13.6	149	M
	4 x13.6	176	H



Figure 9 Adjustable centre of mass by changing middle shelf position, "L," "M," and "H" from left to right

2.3.3 Casters locking conditions

Seven distinct caster locking configurations were tested on the shaking table. These encompassed scenarios of,

1. free rolling, with no locked casters (L0),
2. locking a single caster (L1),
3. locking two casters on the trolley's short side (L2S),
4. locking two casters on the trolley's long side (L2L)
5. locking two diagonal casters (L2D),
6. locking three casters (L3) and
7. the complete lock of all four casters (L4).

Note that for caster 5, locking conditions 6 and 7 are not included during testing as only two of the four casters have brakes. Also, Caster 5, which is commonly found in hospital settings, can lock both the rotation and directions of the wheel.

2.3.4 Wheel and trolley angles

The experiments varied wheel and trolley angles relative to the direction of ground motion, as shown in Figure 10. Six wheel angles were examined, comprising 0 degrees, 45 degrees, 90 degrees, and 180 degrees. Additionally, a hybrid wheel angle configuration was tested, where two casters were set at 0 degrees and two at either 45 or 90 degrees. Please note for the "two swivel+two rigid" caster configurations, the wheel angle only applies to the swivel casters as the rigid caster cannot twist.

Three trolley angles as shown in Figure 10 were tested. Note for simplicity, only the three fundamental configurations with the wheel angle consistently set at 0 degrees to the trolley body are shown in the figure.

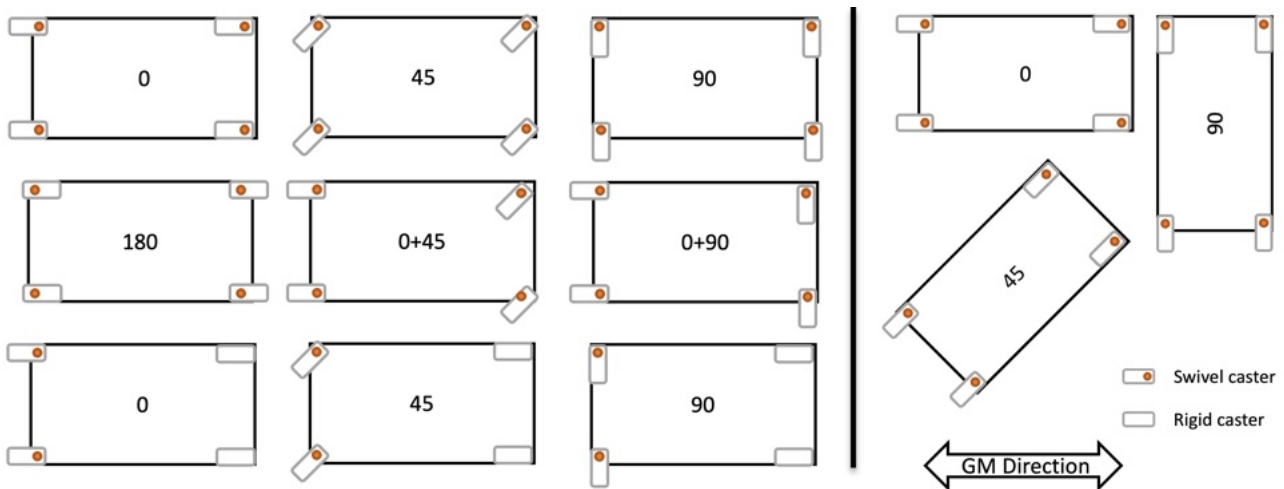


Figure 10 Different wheel angles (left) and trolley angles (right) tested

2.3.5 Ground motions

This study incorporated 16 ground motions, consisting of six sinusoidal ground motions, four sweeping sinusoidal motions, and three earthquake-induced ground motions, each at two intensities. The key parameters for these ground motions are listed in Table 5 and their time histories are plotted in Figure 11. The six sinusoidal ground motions are applied with a ramp in the first 5 seconds.

Table 5 Key parameter of ground motions selected for shake table tests

	Ground motion	a_{max} (g)	v_{max} (mm/s)	d_{max} (mm)	Duration (s)
GM01	Sine, 1Hz, 0.2g	0.20	312	50	60
GM02	Sine, 1Hz, 0.5g	0.50	781	124	60
GM03	Sine, 3Hz, 0.5g	0.50	262	14	60
GM04	Sine, 3Hz, 1g	1.00	520	28	60
GM05	Sine, 5Hz, 0.5g	0.50	156	5	60
GM06	Sine, 5Hz, 1g	1.00	312	10	60
GM07	Sweep sine, f=0.5-2Hz	0.20	624	200	60
GM08	Sweep sine, f=2-0.5Hz	0.20	624	200	60
GM09	Sweep sine, f=2-8Hz	1.00	772	62	60
GM10	Sweep sine, f=8-2Hz	1.00	772	62	60
GM11	Kobe, 50%	0.42	456	105	60
GM12	Kobe, 100%	0.83	911	211	60
GM13	Christchurch, 50%	0.28	283	130	45
GM14	Christchurch, 90%	0.50	510	234	45
GM15	El Centro, 50%	0.14	155	43	54
GM16	El Centro, 100%	0.28	309	87	54

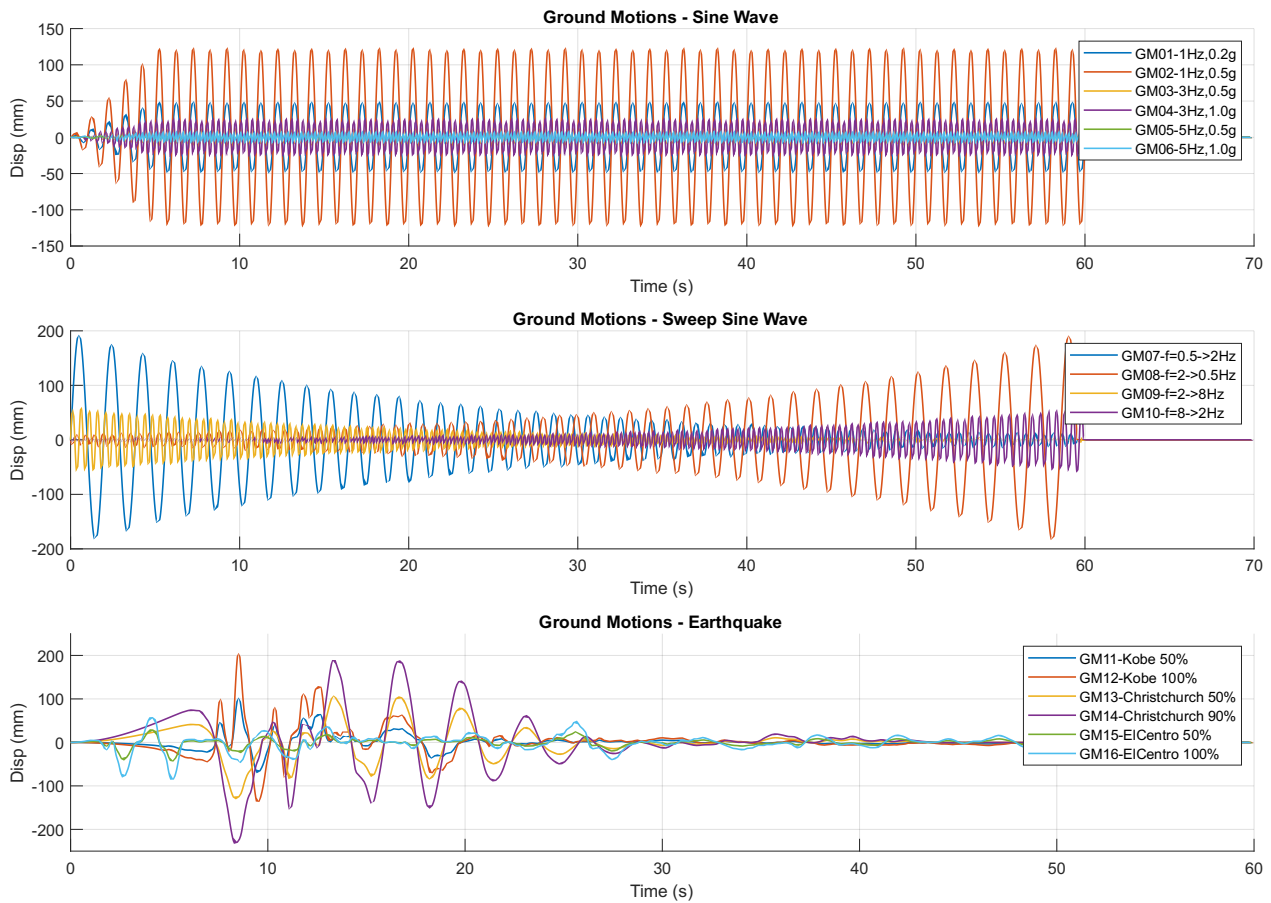


Figure 11 Ground motions selected for shake table testing

3 Results

Preliminary analysis of the results show that the physical setup and the measurement system worked effectively. Further detailed analysis and simulations will be available in future publications. Preliminary observations showed locking casters cause a more severe trolley response, including, large displacement, severe twisting, and rocking motion. Figure 12 shows the absolute displacement of the trolley with one caster locked or free rolling under the same ground motion (GM14 – Kobe 100%). Figure 13 shows x,y planar relative movement of the trolley. More analysis will be underway.

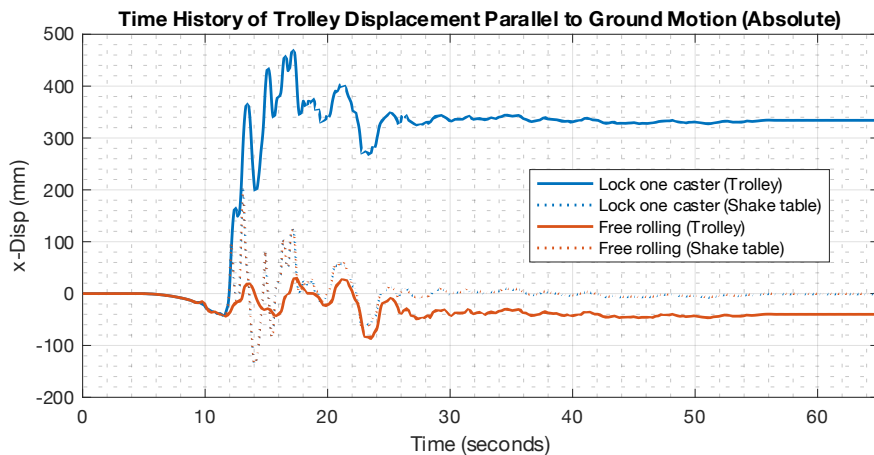


Figure 12 Time history of trolley displacement parallel to ground motion

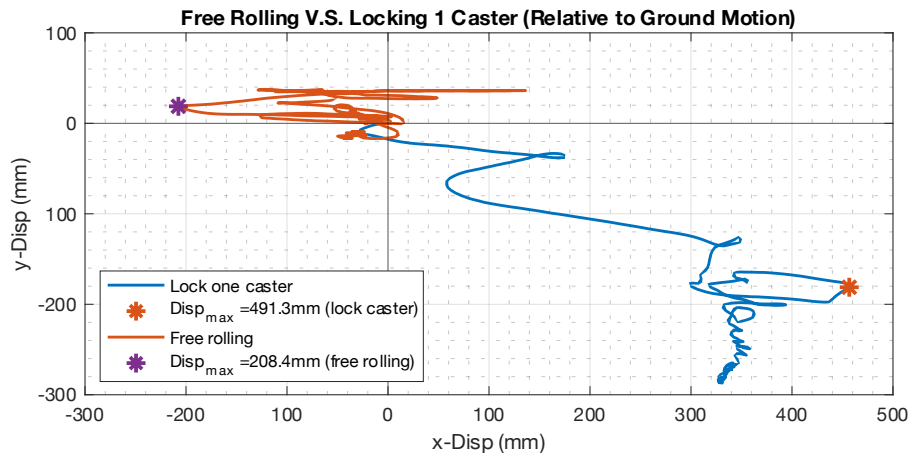


Figure 13 Free rolling V.S. Locking one caster (Relative to ground motion)

4 Summary

This study outlines the experimental design and methodology for a series of shake table tests investigating the factors affecting the seismic response of objects on casters. These tests were designed to replicate the real-world conditions experienced by medical equipment in seismic events. The experiment comprised over 1,300 test runs, carefully capturing the three-dimensional displacements and rotation of both the trolley body and the rolling-and-twisting casters. This data, obtained through a combination of motion capture systems, video recording, and tri-axial accelerometers, will be utilized to analyse the impact of various factors, such as wheel material and sizes, trolley and wheel angles, different self-weight configurations, weight distribution, and seven different locking conditions on the seismic response of medical equipment.

5 Acknowledgment

The authors want to express their gratitude to the AUT technicians for their support during the experimental phase of this research. Sincere thanks to the China Scholarship Council for providing the PhD scholarship for the first author.

6 References

- Baird, A. and Ferner, H. (2017) 'Damage to Non-Structural Elements in the 2016 Kaikōura Earthquake', *Bulletin of the New Zealand Society for Earthquake Engineering*, 50(2), pp. 187–193. Available at: <https://doi.org/10.5459/bnzsee.50.2.187-193>.
- Chai, J.-F. and Lin, F.-R. (2011) 'Seismic Retrofit and Shaking Table Test of Medical Equipment in a Hospital', in. *Ninth Pacific Conference on Earthquake Engineering Building an Earthquake-Resilient Society*, New Zealand. Available at: <https://www.nzsee.org.nz/db/2011/126.pdf>.
- Dhakal, R.P. (2010) 'Damage to Non-Structural Components and Contents in 2010 Darfield Earthquake', *Bulletin of the New Zealand Society for Earthquake Engineering*, 43(4), pp. 404–411. Available at: <https://doi.org/10.5459/bnzsee.43.4.404-411>.
- Dhakal, R.P. et al. (2016) 'Seismic Performance of Non-Structural Components and Contents in Buildings: An Overview of Nz Research', *Earthquake Engineering and Engineering Vibration*, 15(1), pp. 1–17. Available at: <https://doi.org/10.1007/s11803-016-0301-9>.
- Di Sarno, L. et al. (2019) 'Experimental Assessment of the Seismic Performance of Hospital Cabinets Using Shake Table Testing', *Earthquake Engineering & Structural Dynamics*, 48(1), pp. 103–123. Available at: <https://doi.org/10.1002/eqe.3127>.
- Elide Pantoli et al. (2013) *BNCS Report #2: Full-Scale Structural and Nonstructural Building System Performance During Earthquakes and Post-Earthquake Fire – Test Results*. Department of Structural Engineering University of California, San Diego La Jolla, California 92093-008: University of California, San Diego.

- Fajfar, P. and Krawinkler, H. (2004) Performance-Based Seismic Design: Concepts and Implementation ; Proceedings of the International Workshop on, Bled, Slovenia, 28 June - 1 July 2004. International Workshop on Performance Based Seismic Design, Concepts and Implementation, Richmond, Calif: Pacific Earthquake Engineering Research Center, College of Engineering, Univ. of California, Berkeley. Available at: https://peer.berkeley.edu/sites/default/files/0405_edited_by_p._fajfar_and_h._krawinkler.pdf.
- FEMA (2015) Performance of Buildings and Nonstructural Components in the 2014 South Napa Earthquake, Fema P-1024. Washington DC: Federal Emergency Management Agency.
- Filiatrault, A. and Sullivan, T. (2014) 'Performance-Based Seismic Design of Nonstructural Building Components: The Next Frontier of Earthquake Engineering', *Earthquake Engineering and Engineering Vibration*, 13(1), pp. 17–46. Available at: <https://doi.org/10.1007/s11803-014-0238-9>.
- Jacques, C.C. et al. (2014) 'Resilience of the Canterbury Hospital System to the 2011 Christchurch Earthquake', *Earthquake Spectra*, 30(1), pp. 533–554. Available at: <https://doi.org/10.1193/032013EQS074M>.
- Mayer, B.J. and Boston, M. (2022) 'Advancing Nz Hospital Seismic Readiness: Creating a Post-Earthquake Functionality Dashboard'.
- Miranda, E. et al. (2012) 'Performance of Nonstructural Components During the 27 February 2010 Chile Earthquake', *Earthquake Spectra*, 28(1_suppl1), pp. 453–471. Available at: <https://doi.org/10.1193/1.4000032>.
- Mitrani-Reiser, J. et al. (2012) 'A Functional Loss Assessment of a Hospital System in the Bío-Bío Province', *Earthquake Spectra*, 28(1_suppl1), pp. 473–502. Available at: <https://doi.org/10.1193/1.4000044>.
- Myrtle, R.C. et al. (2005) 'Classification and Prioritization of Essential Systems in Hospitals Under Extreme Events', *Earthquake Spectra*, 21(3), pp. 779–802. Available at: <https://doi.org/10.1193/1.1988338>.
- Nikfar, F. and Konstantinidis, D. (2019) 'Experimental Study on the Seismic Response of Equipment on Wheels and Casters in Base-Isolated Hospitals', *Journal of Structural Engineering*, 145(3), p. 04019001. Available at: [https://doi.org/10.1061/\(ASCE\)ST.1943-541X.0002266](https://doi.org/10.1061/(ASCE)ST.1943-541X.0002266).
- OptiTrack (2023) 'Motive'. Available at: <https://optitrack.com/software/motive/>.
- Ornthammarath, T. et al. (2018) 'Observed Hospital Damages Following the 2014 Mae Lao (Northern Thailand) Earthquake: A Survey Report', *Journal of Disaster Research*, 13(4), pp. 804–812. Available at: <https://doi.org/10.20965/jdr.2018.p0804>.
- Suzuki, Y., Fukuda, I. and Nakaji, S. (2014) 'The Operating Room During a Severe Earthquake: Lessons from the 2011 Great East Japan Earthquake', *Disaster Medicine and Public Health Preparedness*, 8(2), pp. 123–129. Available at: <https://doi.org/10.1017/dmp.2014.16>.
- Taghavi, S. and Miranda, E. (2003) Response Assessment of Nonstructural Building Elements. Department of Civil and Environmental Engineering Stanford University: Pacific Earthquake Engineering Research Center (PEER). Available at: https://peer.berkeley.edu/sites/default/files/0305_s._taghavi_e._miranda_.pdf.
- Wang, D., Dai, J. and Ning, X. (2016) 'Shaking Table Tests of Typical B-Ultrasound Model Hospital Room in a Simulation of the Lushan Earthquake', *Bulletin of the New Zealand Society for Earthquake Engineering*, 49(1), pp. 116–124. Available at: <https://doi.org/10.5459/bnzsee.49.1.116-124>.
- Zhang, L. et al. (2012) 'Emergency Medical Rescue Efforts After a Major Earthquake: Lessons from the 2008 Wenchuan Earthquake', *The Lancet*, 379(9818), pp. 853–861. Available at: [https://doi.org/10.1016/S0140-6736\(11\)61876-X](https://doi.org/10.1016/S0140-6736(11)61876-X).